ISBN: 978-3-95450-188-5 doi:10.18429/JACoW-MEDSI2016-WEAA04

NOVEL NUMERICAL METHOD FOR CALCULATING THE SHADOW PROJECTION AND COLLISIONS OF A MULTI-AXIS GONIOMETER AT DIAMOND

V. Grama†, A. Wagner, Diamond Light Source, Didcot, UK

Abstract

Beamline I23 is a long-wavelength macromolecular crystallography beamline at Diamond Light Source. The end station is a unique instrument with a bespoke cryogenically cooled multi-axis goniometer and a large curved Pilatus 12M detector in a high vacuum environment. As experiments become limited by radiation damage to the crystals, optimised strategies are needed to orient crystals in the most efficient way to obtain a complete dataset with a minimal X-ray dose.

Two key factors affect the optimisation strategies. Firstly, shadowing on the detector by the goniometer resulting in data loss in this region and secondly, collisions between the goniometer and other components in the end station restricting the available angular range for sample centering and data collection. This paper discusses the numerical methods for calculating the shadowing of a multi-axis goniometer on a semi-cylindrical detector and the calculation of the allowable angles for various conditions to prevent collisions with neighbouring components.

INTRODUCTION

The long-wavelength macromolecular crystallography (MX) beamline I23 at Diamond Light Source is a unique instrument currently being commissioned. Its main use is to solve complicated protein or nucleic acid structures without additional labelling directly from the naturally occurring sulphur or phosphorus atoms in these macromolecules. To eliminate air absorption at longer wavelengths, the complete end station including the goniometer and detector is in vacuum. As diffraction angles increase at long wavelengths, dedicated solutions for the detector and a multi-axis goniometer have been developed. The detector is a large semi-cylindrical Pilatus 12M area detector developed by Dectris. The multi-axis goniometer in inverse-kappa geometry has been built by the UK Astronomy Technology Centre. It has an $\propto_{\kappa}$ angle of 50° which allows the alignment of crystals along any given crystallographic axis [1].

The samples can be exposed to only a certain amount of radiation dose for data collection before they are damaged. Hence, it is vital to predetermine the most efficient way of orienting the crystal to obtain a complete dataset with minimal X-ray dose.

In order to generate strategies for data collection it is important to know two key factors which affect the optimisation in advance. Firstly, the goniometer kappa head assembly has a fairly large footprint. Because of this, at certain kappa and omega angle combinations the kappa assembly interferes with the projected diffraction leading to shadowing on the detector. This results in a data loss in this region. The shape and location of the shadow is dependent on the orientation of the kappa and omega axes. Secondly, it is important to know what angles are accessible for crystal centering and orienting for data collection. There is a restricted angular range which varies due to potential collisions with other moving components, such as the beamstop, backlight and sample viewing system. These share a common space envelope with the goniometer. Also, it is necessary to generate a collision model to ensure safety during operation since all critical systems operate inside a large vacuum vessel with limited visibility.

SHADOW PROJECTION MODEL

There are six main factors which affect the location and shape of the shadow on the detector –

1. The 3D geometry of the goniometer kappa axis assembly
2. The 3D geometry of the detector
3. The omega angle
4. The kappa angle
5. The XYZ offset on the centering stage
6. The sample position

The global coordinate system for the model is in accordance with the Diamond beamline axis orientation standard. The origin of each axis is at the sample position with the axis arrangement following the right had rule.

- The X axis is horizontal and perpendicular to the beam with the positive direction towards the goniometer.
- The Y axis is vertical with the positive direction being upward.
- The Z axis is horizontal and parallel with the beam with the positive direction being in the direction of propagation of the X-ray beam.

The global coordinate system is shown in Fig. 1.

Goniometer Geometry

The multi-axis goniometer is in inverse-kappa geometry. The main rotational axis or omega (ω) axis has an angular range of ±270°, the secondary kappa (κ) axis

Diamond Light Source, UK
† vinay.grama@diamond.ac.uk

ISBN: 978-3-95450-188-5 doi:10.18429/JACoW-MEDSI2016-WEAA04

has a range of +10° to -190° and the tertiary phi (φ) axis has a range of ± 180°. The kappa and phi axis assembly is mounted on an XYZ stage providing a ±2.5 mm translation in all three axes for centering samples. The XYZ stage is in turn mounted on the omega axis. The angle between the kappa axis and the omega axis is 50° which is defined as the $\propto_\kappa$ angle.

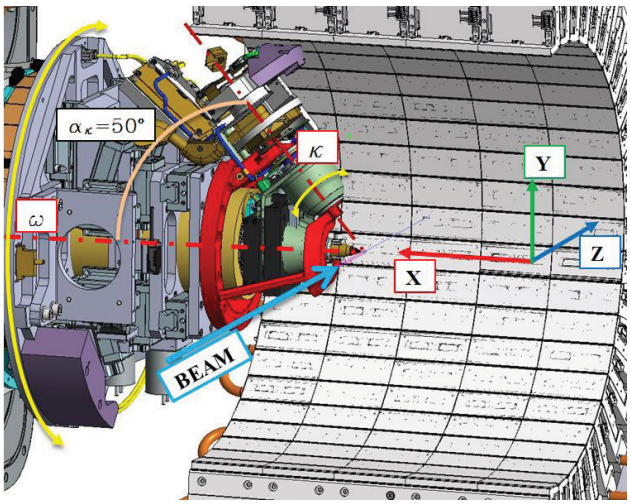

Figure 1: Goniometer coordinate system.

Detector Geometry

The Pilatus 12M detector comprises of 120 modules with 24 banks of 5 modules each arranged in a semi-cylindrical array with the sensor surfaces tangential to a 250 mm diameter cylinder as shown in Fig. 2. The total width of 5 modules on the detector is 424.6 mm. During data collection, the axis of the cylinder is collinear with the omega axis on the goniometer.

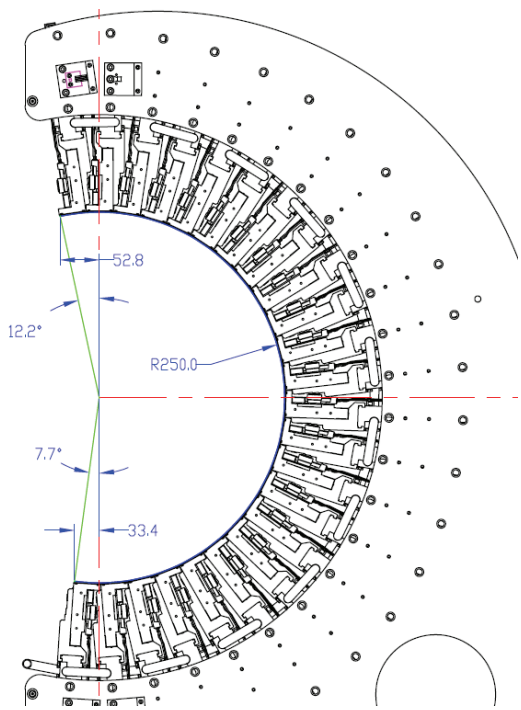

Figure 2: Detector geometry.

Sample Position

There are three possible sample positions along the X-axis direction. These three positions are defined by the combination of the Focussing mirror and Harmonic rejection mirror systems. The goniometer is repositioned in order to align the sample with the beam which results in a shift of the shadowing coordinates in the X direction.

Sample position-1 (default) is considered to have coordinates (0, 0, 0) and is at a distance of 192.3 mm from the outboard end of the detector (goniometer side). Sample position-2 is at (6.4, 0, 0) with reference to Sample position 1 and Sample position-3 is at (-6.4, 0, 0) as shown in Fig. 3.

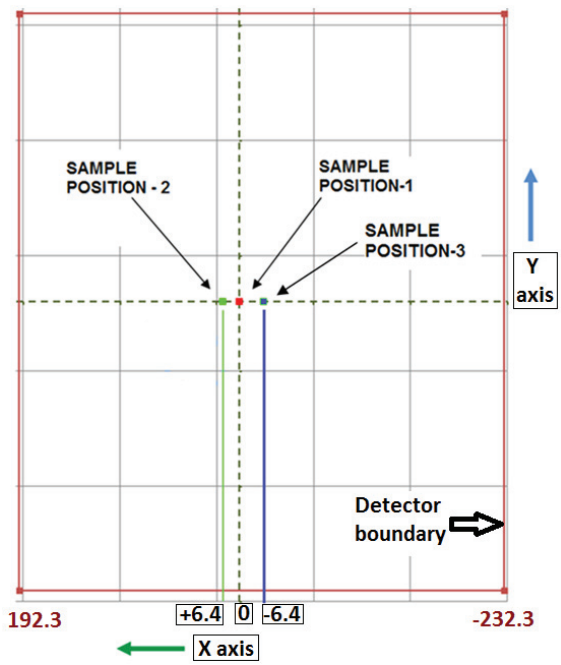

Figure 3: Sample positions (detector shown as red rectangle).

The kappa head assembly was analysed and it was deduced that the shadow on the detector would mainly be due to the outer edge of the kappa assembly. The 3-dimensional coordinates of the outer edge were measured on the CAD model and a 3D profile was generated as shown in Fig. 4.

The coordinate matrix of the profile is given by -

$$C_G = \begin{bmatrix} X_1 & Y_1 & Z_1 \\ \vdots & \ddots & \vdots \\ X_n & Y_n & Z_n \end{bmatrix} \quad (1)$$

These coordinates were then rotated by a defined angle about the kappa axis to obtain a second set of coordinates. The rotation matrix about the kappa axis is expressed as [2] -

$$R_K = \begin{bmatrix} u^2 + v^2 \cos\kappa & uv(1-\cos\kappa) & -v\sin\kappa \\ uv(1-\cos\kappa) & v^2 + u^2\cos\kappa & +u\sin\kappa \\ +v\sin\kappa & -u\sin\kappa & (u^2+v^2)\cos\kappa \end{bmatrix} \quad (2)$$

ISBN: 978-3-95450-188-5 doi:10.18429/JACoW-MEDSI2016-WEAA04

Where,

- κ is the angle about which the 3D profile coordinates are rotated about the kappa axis,
- |u v| is a unit vector of the kappa axis where -

$$u = \cos\ (50^0) \tag{3}$$

$$v = \sin\ (50^0) \tag{4}$$

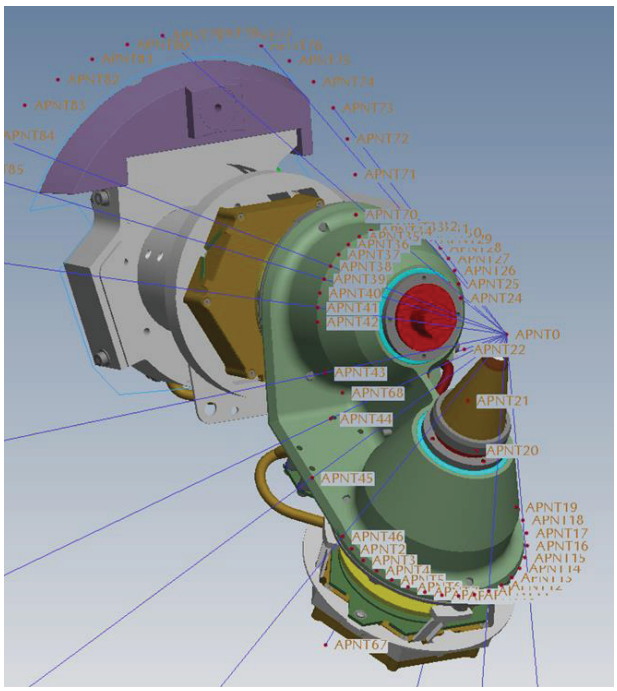

Figure 4: CAD model profile coordinates.

The resulting coordinate matrix is given by:-

$$[C_{KG}] = [C_G] \times [R_K] \tag{5}$$

The coordinates are then offset as a set in the X, Y and Z planes based on the offset from the omega axis for sample centering. This new coordinate matrix $[C_{KO}]$ is then rotated about the Omega axis or global X-axis. The rotation matrix is given by -

$$R_\omega = \begin{bmatrix} 1 & 0 & 0 \\ 0 & \cos\omega & \sin\omega \\ 0 & -\sin\omega & \cos\omega \end{bmatrix} \tag{6}$$

The resulting coordinate matrix is given by -

$$[C_{\omega G}] = [C_{KO}] \times [R_\omega] \tag{7}$$

The coordinates of matrix $[C_{\omega G}]$ are then projected as a ray on to a cylinder of infinite length having a radius equal to 250 mm which is collinear with the Omega axis (X-axis). The rays are defined by the origin (0, 0, 0) and an offset vector given by each set of coordinates (x_i, y_i, z_i) in the matrix $[C_{\omega G}]$. The equation for the projected coordinates is given by [3] -

$$\begin{aligned} x(t) &= t.x_i \\ y(t) &= t.y_i \\ z(t) &= t.z_i \end{aligned} \tag{8}$$

The ray-cylinder or ray-detector intersection is the point with the lowest non-negative value of *t*. The cylinder aligned along the X-axis is defined by -

$$z^2 + y^2 = 250^2 \tag{9}$$

To intersect the ray with the cylinder, equation (8) is substituted in equation (9) to solve for *t* -

$$t = \frac{\pm\sqrt{[-(4(z_i^2 + y_i^2)(-(250^2))]}}{2(z_i^2 + y_i^2)} \tag{10}$$

Since the detector is a partial-cylinder of finite length, the X and Z coordinates are valid if –

- For sample position – 1: -232.3 mm < x < 192.3 mm and z > -52.8 mm (i.e., $-12^0 < \omega < 190^0$)
- For sample position – 2: -238.7 mm < x < 185.9 mm and z > -52.8 mm (i.e., $-12^0 < \omega < 190^0$)
- For sample position – 3: -225.9 mm < x < 198.7 mm and z > -52.8 mm (i.e., $-12^0 < \omega < 190^0$)

The model can be refined for the lower half of the detector geometry by considering the coordinate to be valid for all values of Z greater than -33.4 mm if the Y coordinate of that point is less than zero.

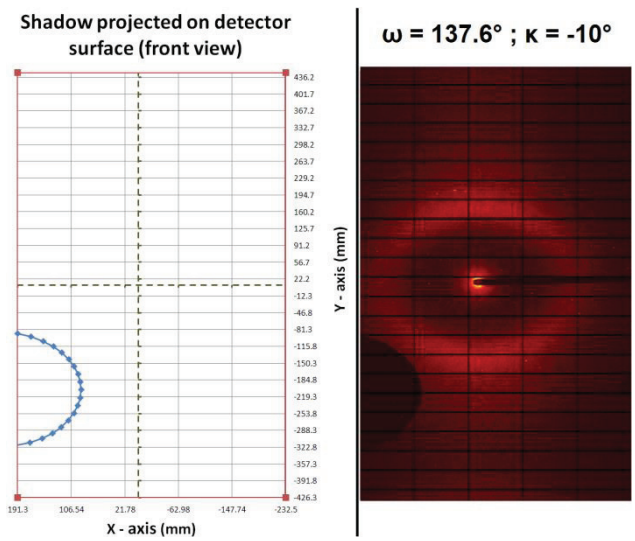

Figure 5: Calculated shadow on detector (left) and recorded shadow (right).

Figure 5 shows a plot of the calculated shadow boundary at ω = 137.6° and κ = -10° against an image recorded on the detector. The calculated profile has been visually compared against the recorded shadow. Detailed analysis is yet to be performed.

ISBN: 978-3-95450-188-5 doi:10.18429/JACoW-MEDSI2016-WEAA04

COLLISION MODEL

The collisions mainly occur between the goniometer kappa assembly and the beam stop, backlight and objective lens during the following two scenarios –

a) During sample centering: collisions between the goniometer kappa axis assembly and the objective lens and backlight.
b) During data collection: collisions between the goniometer kappa axis assembly and the beam stop.

The collision angles are dependent on the following factors –

a) The kappa angle
b) The omega angle
c) The XYZ centering offsets on the goniometer centering stage.
d) The distance of the objective lens from the sample position in the Z direction.
e) The distance of the backlight from the sample position in the Z direction.
f) The distance of the beam stop from the sample position in the Z direction.
g) The geometry of the colliding parts.

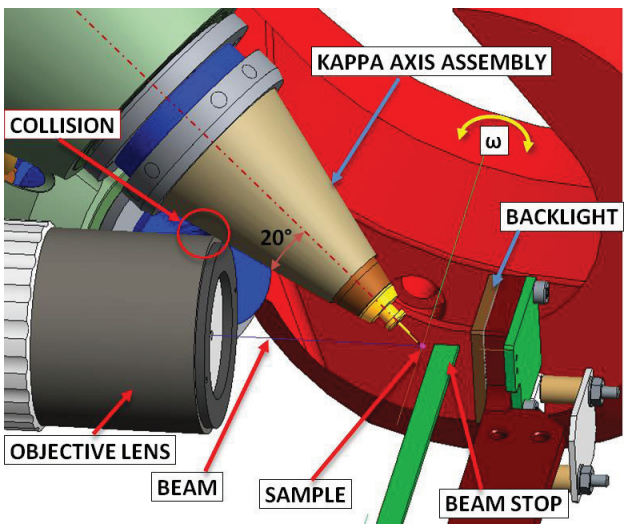

Figure 6: CAD image showing collision between the kappa assembly and objective lens.

Collisions: Kappa Assembly - Objective Lens

The on-axis viewing system allows the visualisation of the sample from the point of view of the beam. The objective lens on the on-axis viewing system has a hole machined through its centre allowing the beam to pass through. During sample centering, the goniometer omega axis is aligned and perpendicular to the beam axis. Also, the objective lens has a diameter of 34 mm with its axis collinear with the beam axis and positioned at a distance equal to its working distance from the sample position. The objective lens can be moved along the Z-axis for into a position which clears all collisions when not being used for sample centering.

The part of the kappa assembly which collides with the objective lens is a cone with a half cone angle of 20° as shown in Fig. 6. The axis of the cone is collinear with the phi axis. In order to predict the collision angles, the problem was simplified to a cone-circle interaction with the apex of the cone at the origin and the circle (front of the objective lens) at a distance of 34 mm from the origin. Theoretically, the vertex of the cone (or sample position) stays at the origin for all kappa and omega angles.

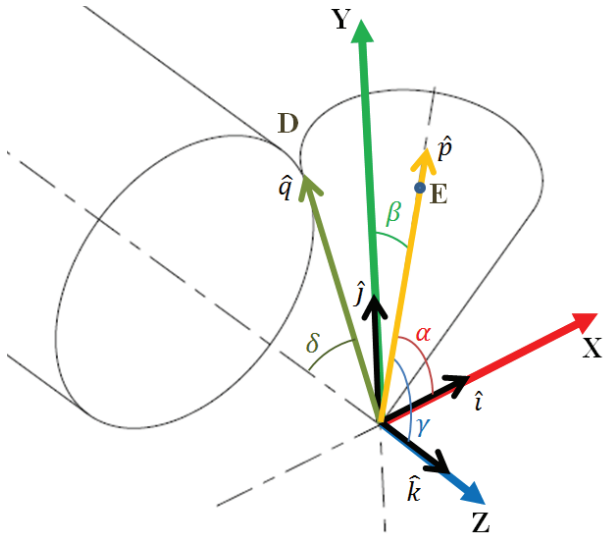

Figure 7: Cone-circle vectors.

Let $\hat{\imath}$, $\hat{\jmath}$ and $\hat{k}$ be unit vectors in the direction of the X, Y and Z axes respectively (Fig. 7). Consider a unit vector $\hat{p}$ directed along the phi axis and the angles between $\hat{p}$ and vectors $\hat{\imath}$, $\hat{\jmath}$ and $\hat{k}$ to be α, β and γ respectively. Let unit vector $\hat{q}$ be directed from the origin to a point D on the circle lying in the $\hat{k} - \hat{p}$ plane and the angle between $\hat{p}$ and $-\hat{k}$ be δ.

In order to calculate the omega angles at which the collisions occur, consider a point E on $\hat{p}$. The centreline of the kappa-cone can be represented as a line joining the origin and point E –

$$A_C = \begin{bmatrix} 0 & 0 & 0 \\ x_E & y_E & z_E \end{bmatrix} \tag{11}$$

The coordinates of point E when rotated about kappa is given by –

$$[A_{KC}] = [A_C] \times [R_K] \tag{12}$$

This new coordinate matrix $[A_{KC}]$ is then rotated about the Omega axis to get the final orientation of the kappa axis cone. The resulting coordinate matrix is given by –

$$[A_{\omega C}] = [A_{KC}] \times [R_\omega] = \begin{bmatrix} 0 & 0 & 0 \\ x_{E1} & y_{E1} & z_{E1} \end{bmatrix} \tag{13}$$

ISBN: 978-3-95450-188-5 doi:10.18429/JACoW-MEDSI2016-WEAA04

Let $\gamma_{\omega C}$ be the angle between the rotated centreline and the unit vector $-\hat{k}$ in the negative direction of the Z-axis. It can be calculate as –

$$\gamma_{\omega C} = \pi - \left(\cos^{-1}\left(\frac{z_{E1}}{\sqrt{(x_{E1}^2 + y_{E1}^2 + z_{E1}^2)}}\right)\right) \quad (14)$$

It can be seen that the kappa assembly collides with the objective lens if $\gamma_{\omega C}$ (in degrees) is less than or equal to δ + 20°. For a given kappa angle, there are two possible omega angles at which the kappa assembly can collide with the objective lens; one at the top of the lens and the other at the bottom. Figure 8 shows the calculated collision between the kappa assembly and objective lens at the same ω & κ angle as shown in Fig. 6.

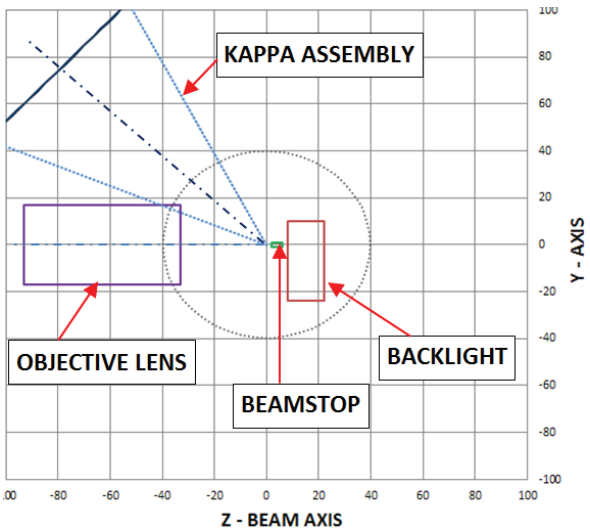

Figure 8: Collision model plotted in 2D.

Collisions: Kappa Assembly - Beam Stop / Backlight

The collisions between the beam stop / backlight and the kappa assembly were simplified and considered to be collisions between a cone and a rectangle.

Let ε be the angle between the Z-axis and the left vertical edge of the beam stop in the horizontal or Y-plane. Also, let ζ be the angle between the Z-axis and the top horizontal edge of the beam stop in the X-plane as shown in Fig. 9.

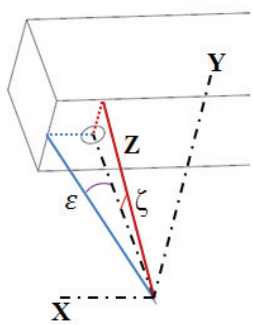

Figure 9: Beam stop: collision angles.

For a given kappa angle, the angle between the kappa cone axis and the X-plane (or α) remains constant for all values of omega. Let $\widehat{p_x}$ be the projection of vector $\hat{p}$ in the X-plane and θ_k be the angle between the projected vector and the Y-axis which is collinear with omega 0°. The omega angles at which the kappa assembly collides with the top edge of the beam stop is, ω_{Bt} = - (ζ + θ_k + 20°) and to the bottom edge is, ω_{Bb} = (ζ - θ_k + 20°). It can said that the kappa assembly collides with the beam stop if both the following conditions are true –

a) If α + 20° is greater than or equal to 90° - ε
b) If omega is between ω_{Bt} and ω_{Bb}

The beam stop is mounted on a linear stage; hence its distance from the sample position varies in Z. However, the collision angles can be easily updated since any change in Z results in a change in angles ε and ζ.

SUMMARY

The shadow model has been visually compared against a set of recorded images and found to be similar. The beamline is still in the early stages of commissioning and detailed analysis of the shadowing data is yet to be performed. This model will be the basis of the crystallographic strategy software currently being developed by Global Phasing Limited, which will take both collisions and shadowing into account.

The collision model was initially verified by manually rotating the kappa and omega axes to different angles in the CAD assembly. Thorough tests have been later performed on the installed system and the model has been found to be accurate. A safety margin of 6 mm has been added to the outer boundary or profile of the objective lens, beam stop and backlight to accommodate for the centering offsets and minor misalignments.

The model has been easily adapted for calculating the shadowing of other goniometers such as the SmarGon on standard detectors with flat surfaces at Diamond.

ACKNOWLEDGEMENT

We would like to thank the team of engineers, scientists and technicians mainly Ramona Duman, Dave Butler, Kamel El Omari and Vitaliy Mykhaylyk for their extensive support during collision testing.

REFERENCES

[1] A. Wagner, R. Duman, K. Henderson and V. Mykhaylyk, "In-vacuum long-wavelength macromolecular crystallography", *Acta Cryst.*, D72, p. 430-439, Jan. 2016.

[2] Rotation About an Arbitrary Axis in 3 Dimensions, http://inside.mines.edu/fs_home/gmurray/ArbitraryAxisRotation

[3] Ray tracing primitives, http://www.cl.cam.ac.uk/teaching/1999/AGraphHCI/SMAG/node2.html